International Journal of Geo-Information

MDPI

Article

Toward Quantifying Interpolation Uncertainty in Set-Line Spacing Hydrographic Surveys

Elias Adediran [1], Christos Kastrisios [1,*], Kim Lowell [1], Glen Rice [2] and Qi Zhang [3]

[1] Center for Coastal and Ocean Mapping/UNH-NOAA Joint Hydrographic Center, University of New Hampshire, Durham, NH 03824, USA; elias.adediran@unh.edu (E.A.); klowell@ccom.unh.edu (K.L.)
[2] U.S. Department of Commerce, National Oceanic and Atmospheric Administration, Office of Coast Survey, Hydrographic Systems and Technology Branch, Silver Spring, MD 20910, USA; glen.rice@noaa.gov
[3] Department of Mathematics and Statistics, University of New Hampshire, Durham, NH 03824, USA; qi.zhang2@unh.edu
* Correspondence: christos.kastrisios@unh.edu

Abstract: The oceans remain one of Earth's last great unknowns, with about 74% still unmapped to modern standards. Consequently, interpolation is employed to create seamless digital bathymetric models (DBMs) from incomplete hydrographic datasets, but this introduces unquantified depth uncertainties. This study aims to estimate and characterize uncertainties arising from set-line spacing hydrographic surveys, which are important for nautical charting, navigational safety, and many other applications. By sampling four distinct complete-coverage testbeds in United States waters that vary in slope and roughness at different line spacings, this study interpolates across entire testbed areas using Spline, Inverse Distance Weighting, and Linear interpolation. Uncertainty is calculated by comparing interpolated depths against the source depths for independent points. The resulting interpolation uncertainties are evaluated from both scientific and operational perspectives. Linear regression and machine learning techniques, specifically artificial neural networks and random forest, are used to model the relationship between these uncertainties and three ancillary predictors (distance to the nearest known measurement, slope, and roughness) for interpolation uncertainty quantification. The results show operational equivalence among the three interpolators, how line spacing and morphology impact uncertainty, and the statistical significance of the examined uncertainty predictors. However, the relationships between the combined ancillary predictors and interpolation uncertainty are weak. These findings suggest the potential presence of unaccounted-for factors influencing uncertainty yet provide a foundational understanding for improving uncertainty estimates in DBMs within operational settings.

Keywords: hydrography; set-line spacing surveys; survey designs; interpolation; digital bathymetric models; uncertainty estimation; geospatial analysis; machine learning; nautical charting

Academic Editor: Wolfgang Kainz

Received: 7 November 2024
Revised: 24 December 2024
Accepted: 2 January 2025
Published: 18 February 2025

Citation: Adediran, E.; Kastrisios, C.; Lowell, K.; Rice, G.; Zhang, Q. Toward Quantifying Interpolation Uncertainty in Set-Line Spacing Hydrographic Surveys. *ISPRS Int. J. Geo-Inf.* **2025**, *14*, 90. https://doi.org/10.3390/ijgi14020090

1. Introduction

The Earth's oceans, constituting approximately 71% of its surface [1], remain one of our planet's last great unknowns. Surprisingly, the surfaces of Mars, Venus, and the Earth's Moon are mapped at a higher spatial resolution than the seafloor [2], where individual depth measurements can exhibit data gaps spanning hundreds of kilometers [3]. While efforts are ongoing to completely map the global seafloor by 2030 [4], about 74% of the world's ocean are still unmapped to modern standards [5].

These bathymetric data gaps can be the result of survey designs lacking resources for complete-seabed-coverage hydrographic surveys, or survey oversight, and can span meters to kilometers between survey measurements. The former is still the major cause of the bathymetry data gaps in the ocean, and this is as a result of the considerable time and resources (and therefore costs) associated with the acquisition of high-resolution bathymetric data [6].

Modern bathymetric data can be acquired through various methods and instruments, including single-beam echo-sounders (SBESs) [7], multibeam echo-sounders (MBESs) [8,9], phase-difference side-scan sonar [10], Light Detection and Ranging (LiDAR) [11], satellite-derived bathymetry (SBD) [12], satellite altimetry [3], and crowdsourced bathymetry [13]. Each method has its own advantages and disadvantages in terms of cost, accuracy, resolution, coverage, repeatability, and depth limitations. The present work focuses on high-resolution bathymetric surveys obtained using instruments that transmit acoustic signals through water, such as SBESs and MBESs. This method of data acquisition leads to different types of survey designs used to achieve different types of seafloor coverage.

According to the National Oceanic and Atmospheric Administration (NOAA) Hydrographic Survey Specifications and Deliverables (HSSD) 2022, there are four classifications of coverage: object detection coverage, complete coverage, set-line spacing, and track line (transit and reconnaissance) [14]. The choice of coverage determines the appropriate hydrographic survey technique to employ. Object detection coverage is applied in critical areas requiring under-keel clearance. It involves achieving complete bathymetric coverage using MBESs with object detection capabilities, typically with a 50 cm grid resolution in the 0–20 m depth range [14].

Complete coverage is employed in areas that, while less stringent than those requiring object detection, are still important for identifying navigational hazards. This classification requires full bathymetric coverage using MBESs designed for complete-coverage surveys, with a 1 m grid resolution in the 0–20 m depth range [14]. Complete bathymetric coverage ensures depth measurements are taken across the entire survey area with appropriate line spacings, leaving no significant portions of the seabed unsampled. This enables the detection of potential hazards and provides an accurate representation of the seafloor topography. The set-line spacing hydrographic survey technique, which is the focus of this work, uses SBESs or MBESs to survey an area with specified line spacings that do not achieve full bathymetric coverage. This technique is primarily used in areas too shallow for efficient full-bottom-coverage bathymetry or too hazardous for SBES or MBES deployment [14]. Hydrographic offices worldwide, such as NOAA's Office of Coast Survey (OCS), rely on set-line spacing hydrographic survey techniques to cover large areas relatively quickly and at reduced cost, albeit with the drawback of incomplete bathymetric data coverage. Consequently, interpolation becomes an essential step to fill in data gaps among set-line spacing survey bathymetric datasets and to create a seamless digital bathymetric model (DBM) of the seafloor for numerous scientific and commercial applications.

Interpolation is a mathematical process used to predict unknown values based on surrounding measured values, under the assumption that the surface is continuous and smooth and that measured values at neighboring points are highly correlated with the value at the unknown point [15,16]. Various interpolation methods exist, all of which assume that bathymetry is positively spatially autocorrelated, in line with Tobler's First Law of Geography [17]. This study examines three commonly employed deterministic interpolation techniques—Linear, Spline, and Inverse Distance Weighting (IDW). These methods were selected due to their ubiquity, simplicity, and computational efficiency, which makes them suitable in an operational setting. On the contrary, geostatistical methods like Kriging were excluded due to their computation- and time-intensive nature. For a

detailed explanation of the investigated interpolation methods and the general classes of interpolation methods, see [18].

Beyond creating a DBM with these interpolation methods, there is a crucial need to inform users of the confidence in the data within the interpolated regions, as the interpolation process introduces depth uncertainty of unknown nature into the DBM. Although geostatistical methods (e.g., see [19–21]) provide uncertainty estimates, their computational demands render them unsuitable for this research. This study aims to produce data-driven operationally viable hydrography products from large national datasets while assigning appropriate hydrographic quality metrics of uncertainty. Therefore, it focuses on investigating deterministic spatial interpolation methods for uncertainty quantification in set-line spacing surveys using methods that can be applied in operational settings. Additionally, it characterizes the uncertainty by relating it to measurable seafloor characteristics such as slope and roughness.

Uncertainty in bathymetric models generated from interpolated datasets is particularly important for hydrographic data collection, nautical charting, navigation safety, and modeling purposes [18]. The International Hydrographic Organization (IHO) S-44 defines the standards applicable to hydrographic surveys and sets minimum standards to be achieved. S-44 describes the orders of safety of navigation surveys that are considered acceptable for the production of navigational products and services to enable surface vessels to navigate safely [22]. As requirements may vary, five different survey orders are defined to cater for a different range of needs. These orders include Order 2, Order 1b, Order 1a, Special Order, and Exclusive Order (see [22] for more information on each order).

It is important to note that the S-44 hydrographic survey order is one of the input parameters in determining the data quality requirements for final nautical charting products. Other parameters include factors such as cartographic generalization, gridding, etc. The IHO defines the data quality requirements for charting purposes through the Category of Zones of Confidence (CATZOC) levels and the Quality of Bathymetric Data (QoBD) in the S-57 IHO Transfer Standard for Digital Hydrographic Data [23] and in the new S-101 ENC Product Specification [24], respectively. CATZOC/QoBD, in general, addresses three types of uncertainty—positional, depth, and features (that may create navigation hazards)—and is an indicator that a particular survey meets the minimum criteria for these accuracy parameters based on specific standards (Table 1).

This study aims to facilitate the a posteriori CATZOC classification of interpolated datasets in areas where set-line spacing survey techniques were deployed. This includes addressing the uncertainty metric associated with depth accuracy in CATZOC, excluding, however, considerations of seafloor feature detection and factors like expected feature size or seabed undulations. Thus, possible CATZOC classification improvement through the better estimation of interpolation uncertainty is generally limited to CATZOC B unless the hydrographic offices' full-seabed-coverage and feature detection requirements for CATZOC A1 and A2 are met using side-scan sonar. This study aims to illuminate how interpolation uncertainty can be used to optimize 'on-the-fly' set-line spacing hydrographic survey design to meet a targeted survey order/CATZOC within the constraints of existing resources, thereby making field data collection more efficient and effective.

Despite the critical importance of uncertainty associated with interpolation-based bathymetry generated from set-line spacing surveys, there is little to no research on characterizing and estimating interpolation uncertainty in set-line spacing surveys within the field of ocean mapping. For example, Adediran et al. [18] investigated estimating interpolation uncertainty in sparse bathymetric datasets which is only relevant for archival bathymetric datasets. However, they did not consider the modern systematic data collection of set-line spacing hydrographic survey. In light of this gap, building upon the methods and findings

of the aforementioned work ([18]), this study aims to estimate the interpolation uncertainty in set-line spacing hydrographic surveys and explore how this uncertainty can help inform set-line spacing survey design.

Table 1. The International Hydrographic Organization (IHO) S-57 Category of Zones of Confidence (CATZOC) levels and S-101 Quality of Bathymetric Data (QoBD). Depth and position accuracies are at a 95% confidence interval [25]. (d is water depth in meters.)

CATZOC LEVEL	QoBD	POSITIONAL ACCURACY	DEPTH ACCURACY	SEAFLOOR COVERAGE
A1	1	5 m + 5% d	0.5 m + 1% d	Full area search undertaken. Significant seafloor features detected, and depths measured.
A2	2	20 m	1 m + 2% d	Full area search undertaken. Significant seafloor features detected, and depths measured.
B	3	50 m	1 m + 2% d	Full area search not achieved; uncharted features; hazardous surface navigation is not expected but may exist.
C	4	500 m	2 m + 5% d	Full area search not achieved; depth anomalies may be expected.
D	5	Worse than CATZOC C	Worse than CATZOC C	Full area search not achieved, large depth anomalies may be expected.
U	6	Unassessed	Quality of data has yet to be assessed	
	O	Oceanic	Oceanic areas with water depth greater than 200 m	

In detail, this research aims to address the following questions:

1. Which deterministic interpolation method yields the lowest interpolation uncertainty for set-line spacing survey bathymetry?
2. How efficiently can distance to the nearest known measurement, seabed slope, and roughness be used to estimate and characterize interpolation uncertainty in bathymetric models in an operational setting?
3. To what extent can we improve depth interpolation uncertainty estimation by employing machine learning techniques to combine the above predictors?

Estimating and characterizing interpolation uncertainty in set-line spacing hydrographic surveys is not only important for improving the filling of bathymetric gaps but also for improving the quality of bathymetry by assigning associated quality metrics to bathymetric data. It is also significant for improving the effectiveness and efficiency of hydrographic surveys by reducing the time and cost of surveys while meeting the targeted survey order/CATZOC. This makes the work important to the entire hydrographic community for the safety of navigation, shipping route optimization, survey planning, and associated cost savings.

It is also of great relevance to many ongoing NOAA data-driven projects, such as the National Bathymetric Source Program [26], which are cornerstones of safer navigation, resilient coastal communities and ecosystems, and a stronger blue economy through the sustainable use and management of ocean resources for economic growth.

The subsequent sections of this paper are structured as follows: Section 2 details the datasets and methods employed, Section 3 presents the obtained results on four testbeds, Section 4 engages in a comprehensive discussion of the findings, and Section 5 offers concluding remarks.

2. Materials and Methods

This section provides a description of the study areas under investigation and the datasets employed. Furthermore, it defines the predictors and outlines the methodologies employed to accomplish the specified objectives.

2.1. Testbeds and Datasets

Four distinct bathymetric surfaces were strategically chosen as testbeds within U.S. waters to represent diverse seafloor morphologies, as illustrated in Figure 1. These testbeds, each measuring 10 km by 10 km with an 8 m pixel resolution, encompass varying combinations of slope and roughness characteristics, enabling a thorough analysis of factors that may impact interpolation uncertainty. For a detailed overview of the testbeds, including their names, morphology, respective locations, and key attributes, refer to Table A1.

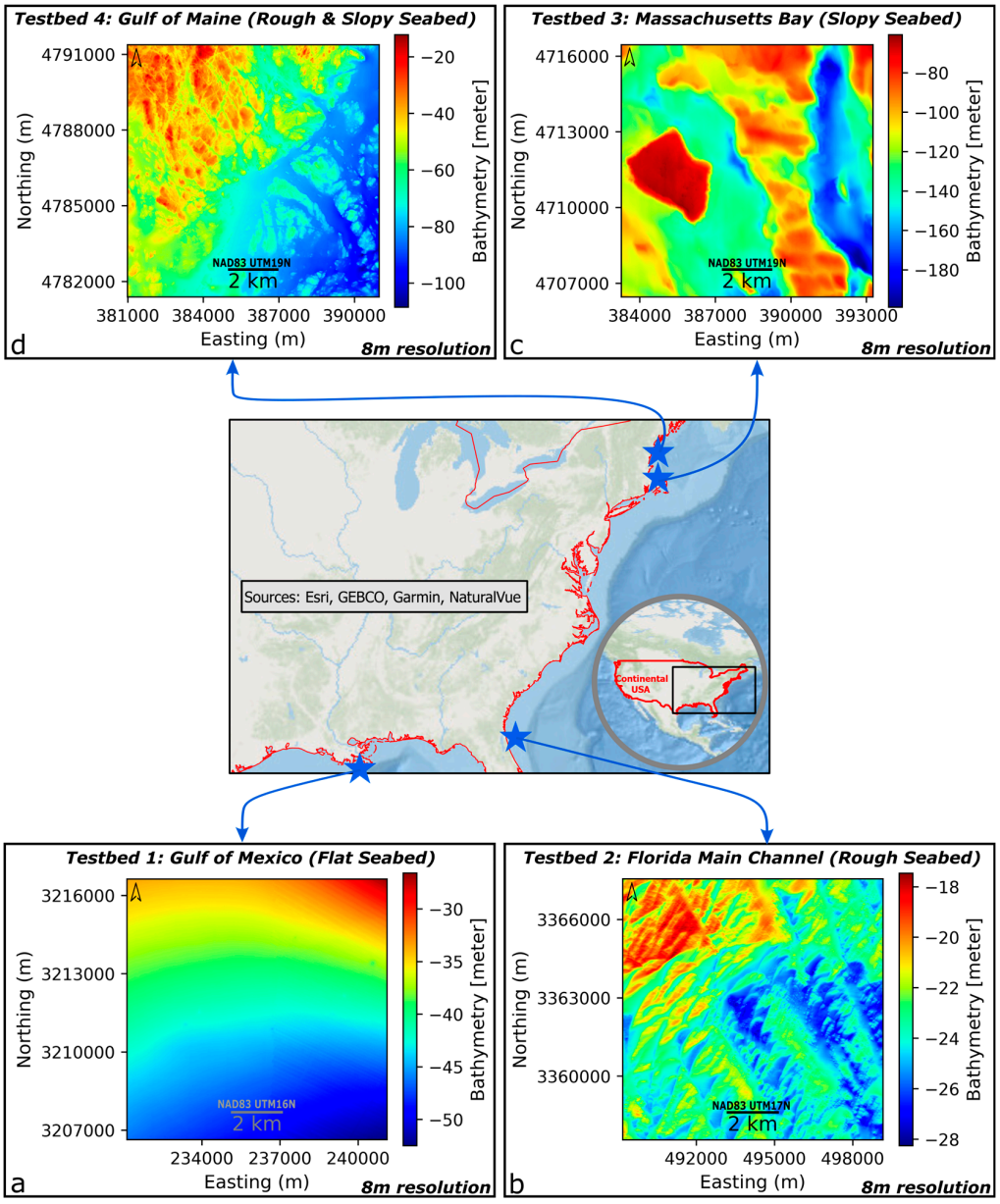

Figure 1. Four testbeds of various seabed characteristics for testing the proposed methodology in (**a**) Gulf of Mexico (flat seabed), (**b**) Florida main channel (rough seabed), (**c**) Massachusetts Bay (slopy seabed), and (**d**) Gulf of Maine (rough and slopy seabed) Adapted with permission from ref. [18] Copyright 2024 Taylor & Francis Ltd.

The bathymetric datasets for these testbeds shown in Figure 1 were sourced from NOAA's BlueTopo repository, horizontally referenced to their respective North American Datum of 1983 (NAD83) and Universal Transverse Mercator (UTM) zone (Table A1), and vertically referenced to North American Vertical Datum 1988 (NADV88), positively upward. The BlueTopo repository offers both raw and interpolated bathymetry; great care was taken to exclusively utilize raw data that had not been subjected to interpolation. These non-interpolated BlueTopo depths are designated as the "true depth" despite any uncertainty associated with these measurements. Following the dual-assessment approach in [18], the selected testbeds were evaluated for an accurate representative of their respective seabed morphologies using qualitative visualization inspection and quantitative analysis, i.e., the slope and roughness histograms presented in Figure 2.

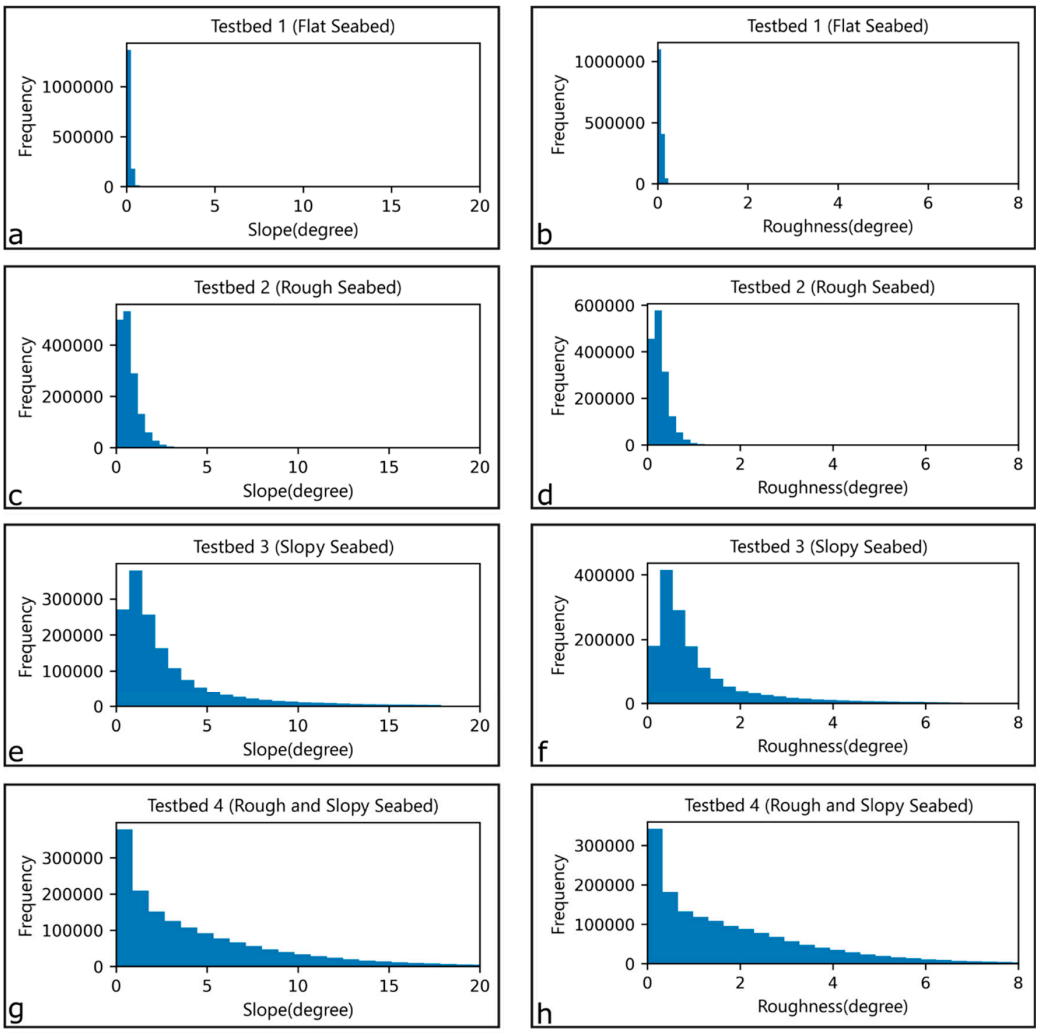

Figure 2. Histograms depicting the slope and roughness characteristics of the original testbeds' bathymetric datasets (e.g., (**a**) depicts the histogram of the slope of Testbed 1 (**b**) depicts the histogram of the roughness of Testbed 1 (**c**) depicts the histogram of the slope of Testbed 2 (**d**) depicts the histogram of the roughness of Testbed 2 (**e**) depicts the histogram of the slope of Testbed 3 (**f**) depicts the histogram of the roughness of Testbed 3 (**g**) depicts the histogram of the slope of Testbed 4 (**h**) depicts the histogram of the roughness of Testbed 4). Reprinted with permission from ref. [18] Copyright 2024 Taylor & Francis Ltd.

In comparing the slope and roughness values across the testbeds, the histograms demonstrate that the testbeds capture their respective morphologies. Terrain characteristics of slope and roughness in the context of this work are defined in the following section.

2.2. Terrain Characterization

This study focused on two key terrain characteristics, specifically slope and roughness, to evaluate how seabed morphology influences uncertainty estimation. These predictors were chosen based on their relatively high correlation with interpolation uncertainty, as revealed by preliminary analysis. Other terrain characteristics including curvature and aspect were excluded due to their low correlation with uncertainty. The following sections provide a detailed explanation of the definitions of slope and roughness and the methodology used to calculate these predictors in the context of this work.

2.2.1. Slope

Slope represents the steepest rate of depth variation within a moving analysis window t is calculated using the gradients in both the X (fx) and Y (fy) directions, as shown in Equation (1):

$$\text{Slope} = \arctan\left(\sqrt{(fx)^2 + (fy)^2}\right) \quad (1)$$

To calculate slope (or other terrain characteristics like roughness), an analysis window moves across the raster DBM surface. Each pixel then acts as the central point for computations (Figure 3).

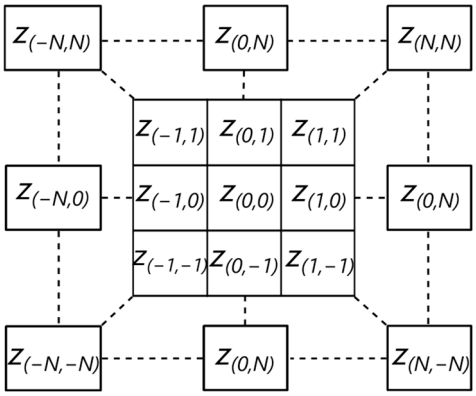

Figure 3. An n × n analysis window for a raster grid. Reprinted with permission from ref. [18] Copyright 2024 Taylor & Francis Ltd.

This generalization allows the predictor to be examined at various scales (different values of n ≥ 3) [27]. Notably, this study utilizes a 3-by-3 window size, as preliminary comparisons with 5-by-5 and 7-by-7 windows showed similar outcomes. This finding aligns with [18], which, using a random sampling approach, reported no significant differences in estimating interpolation uncertainty among the three window sizes (3-by-3, 5-by-5, and 7-by-7). Horn's finite difference method [28] is employed to calculate the fx and fy of the central point of the analysis window using appropriate convolution kernels. Horn's technique uses convolution kernels specifically designed for each moving analysis window to estimate a value for a subject pixel [28].

2.2.2. Roughness

Roughness quantifies the variation in elevation within a given sampled terrain unit and captures both highs and lows. The definition of terrain surface roughness is dependent on the scale considered, and the unit of measurement across a scale window is crucial. This research employs the roughness calculation method outlined by [27]. This approach determines roughness by identifying the maximum difference in elevation between a central cell and its adjacent cells within an n × n rectangular neighborhood (see Figure 3 for illustration). In this study, the 3-by-3 window size is employed.

2.3. Interpolation Techniques

This study quantified uncertainty in interpolated bathymetric datasets generated from three common deterministic interpolation techniques, i.e., IDW, Spline, and Linear, across four distinct testbeds in the United States. The algorithms for these interpolators were developed in Python such that minimal adjustment of interpolation parameters was required. This deliberate approach aims to streamline the implementation process and enhance the applicability of the developed algorithms, thereby eliminating dependence on specific GIS software. Consequently, the optimization of interpolation parameters was not within the scope of this work, and the optimal IDW parameters identified in [29] were employed.

2.4. Implementation of Methodology

The methodology utilized herein was the simulation of set-line spacing surveys from the testbeds' complete-coverage depth measurement (Figure 4) and investigation of uncertainty estimation associated with interpolation within this known area. The main line spacings used were 16 m, 32 m, 64 m, 128 m, 256 m, and 512 m. These line spacings were chosen to understand how interpolation uncertainty will behave in relatively small and wide line spacings. Since main lines are usually supplemented by cross lines to verify and evaluate the internal consistency of hydrographic surveys, the set-line spacing surveys' cross line spacings were calculated using 9% of the main line mileage according to [14] and distributed geographically across the testbeds; see Figure 4 for an example. The set-line survey was simulated across each testbed using these main line spacings and their appropriate cross line spacings.

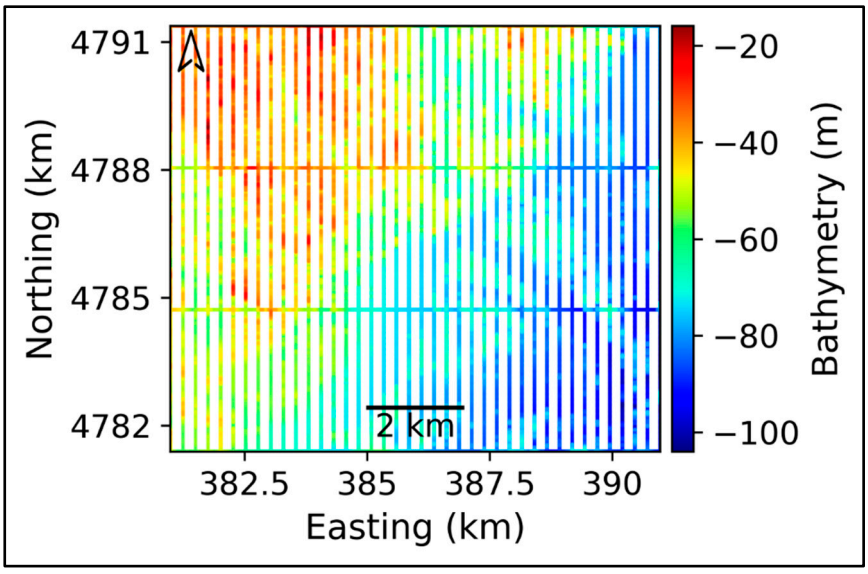

Figure 4. Example of a simulated set-line spacing explored in this study: 256 m main line spacing and equivalent cross line spacing training depths on Testbed 4.

Depths along the main and cross lines, selected using the main line and calculated cross line spacing, were designated as training depths for interpolation. The unselected depths, referred to as test depths, were earmarked for uncertainty quantification and error analysis. See Figure 5 for a schematic of the data preparation and analysis workflow.

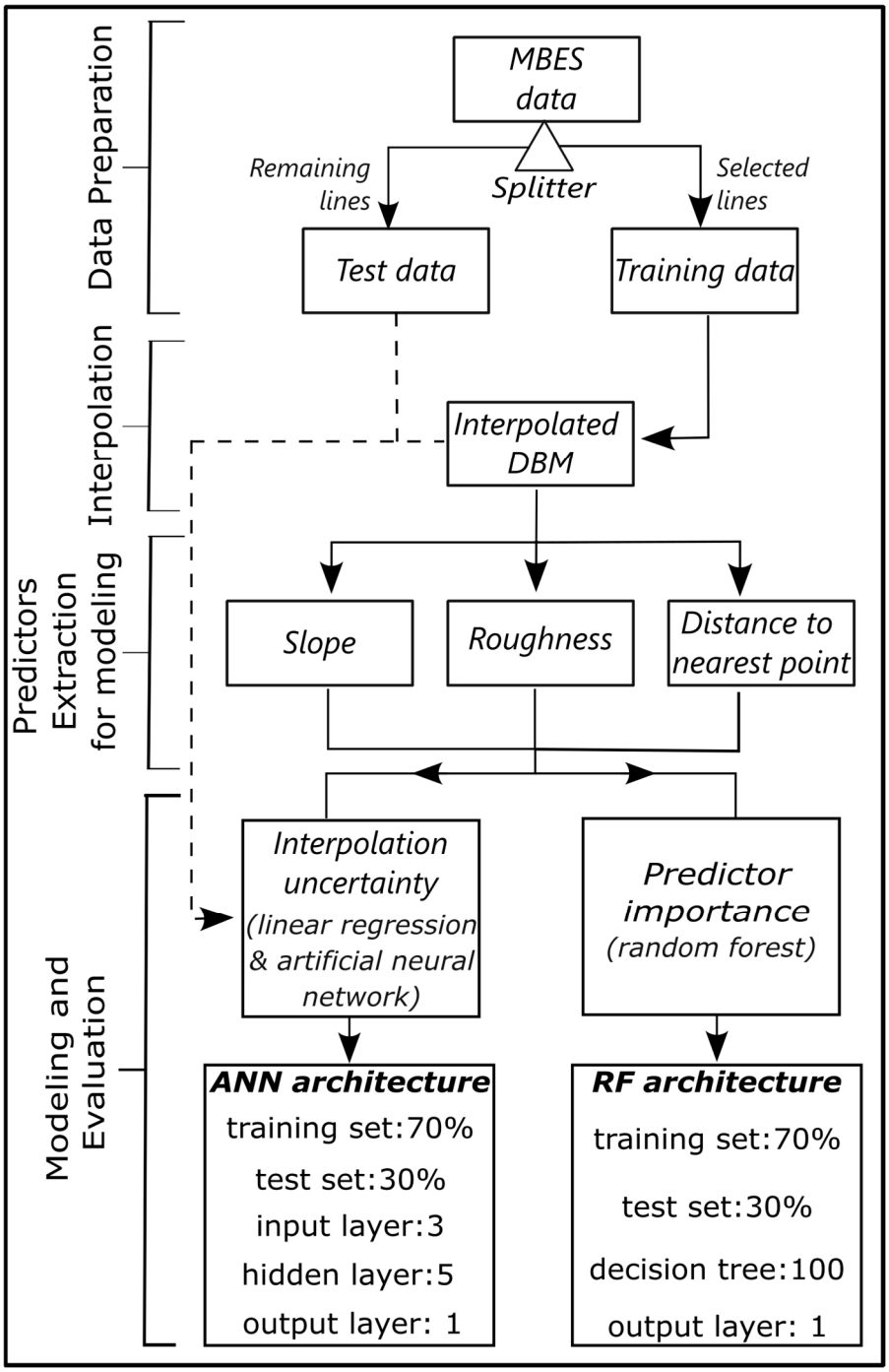

Figure 5. Workflow for quantifying interpolation uncertainty in set-line spacing surveys, including the machine learning techniques' architectures.

The training depths were interpolated using each of the interpolation techniques employed. The resulting interpolated raster was then compared, on a cell-by-cell basis, to the test depths to quantify interpolation uncertainty. Interpolation uncertainty was determined as the absolute value of the difference between the interpolated depths and the measured depths for the cells that were in the test dataset and not within one of the set lines. Ancillary predictors, such as the Euclidean distance to the nearest known measurement and the slope and roughness raster surfaces were generated from the training depths and the interpolated DBM, respectively (refer to Figure 6). These predictors, along with their respective interpolation uncertainties, constituted the datasets prepared for modeling to discern the relationship between the predictors and interpolation uncertainties to quantify

the 'estimated uncertainty' and determine the most important predictor(s) of interpolation uncertainty. To mitigate bias in the analysis, depth measurements along the border of study areas were part of the data used for interpolation. This approach minimized potential edge effects by ensuring that the interpolated values near the study area's boundaries were influenced by actual measured depths, reducing potential inaccuracies that could arise from extrapolation.

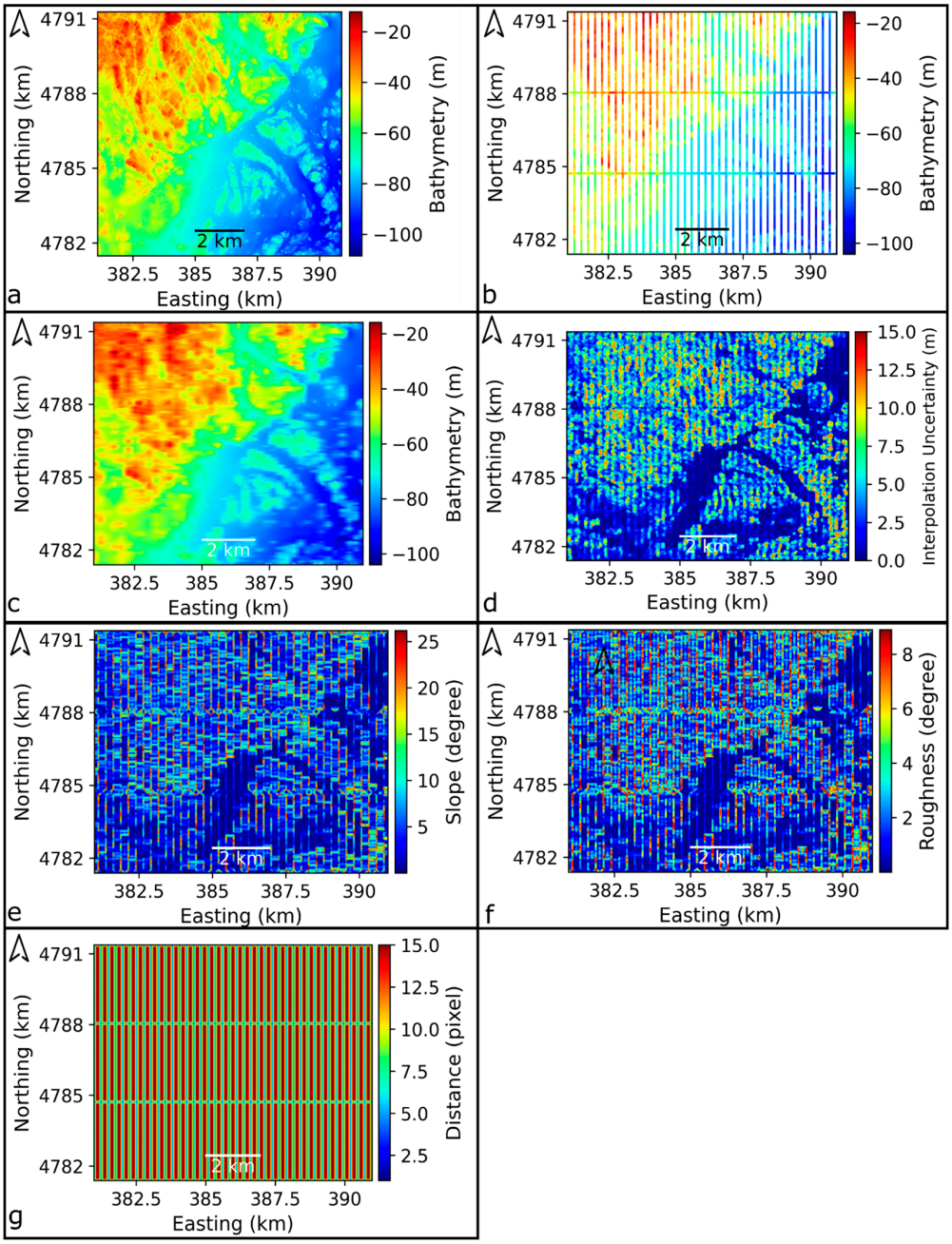

Figure 6. Testbed 4: (**a**) measured depth, (**b**) 256 m main line spacing and equivalent cross line spacings training depths, (**c**) linear interpolated depths, (**d**) interpolation uncertainty clipped to 99 percentile, (**e**) generated slope from interpolated depths, (**f**) generated roughness from interpolated depths, and (**g**) distance to the nearest known measurement raster.

2.5. Modeling and Analysis

Linear regression was employed to model the relationship between interpolation uncertainty and individual predictors, resulting in an estimated uncertainty. For each testbed,

linear regression models were created for three predictors—distance to the nearest known measurement, slope, and roughness—separately for all line spacings and interpolation methods. The performance of these models was measured using the adjusted coefficient of determination (R^2) and root mean square error (RMSE) in meters.

To move beyond individual predictor effects, this study used artificial neural networks (ANNs) (see [30]) to capture nonlinear relationships, interactions, and hidden patterns among the combined predictors. These capabilities surpass traditional methods such as multivariate regression, which may not adequately identify such complexities. Random forest (RF) techniques were employed to assess the importance of uncertainty predictors due to their computational efficiency compared to identifying predictor importance using the ANN's SHAP (SHapley Additive exPlanations) (see [31]), which is computationally expensive. RF was used to complement the ANN model in order to explain which predictor is most important for predicting interpolation uncertainty. Both the ANN and RF models' architectures are summarized in Figure 5.

The ANN was implemented in Python using the Keras library with a TensorFlow backend. The dataset was split into 70% training data and 30% test data, and standard scaling normalization was applied to both sets. The model architecture included an input layer with 10 neurons, a hidden layer with five neurons using the Rectified Linear Unit (ReLU) activation function [32], and an output layer with one neuron employing linear activation for regression tasks. The training involved specifying the mean squared error (MSE) as the loss function, using the Adam optimizer for gradient descent [33], and monitoring the mean absolute error (MAE) during five epochs of training. The model predicted interpolation uncertainty for the test data, and performance was assessed using an adjusted R^2 and RMSE.

The RF implementation in Python utilized the Scikit Learn Random Forest Regressor. Similarly to the ANN, the data were split into training and testing sets and normalized. An RF model with 100 decision trees was created and trained on the normalized training data. Performance evaluation metrics included the adjusted R^2 and RMSE. The importance of each predictor in the model's prediction was assessed, considering the number of trees in which a variable appeared.

To determine the significance of variable contributions to models, a non-parametric bootstrap approach was used. The RF model was fitted to 500 bootstrapped datasets of about 120,000 data points, and the resulting variable importance values from each RF model were combined to compute the mean importance and 95% confidence intervals. In averaging across all line spacings and interpolation methods, the overall mean importance and 95% confidence intervals for each variable were computed.

By employing both ANN and RF methods, this study combined robust prediction and interpretability, enabling a comprehensive understanding of the drivers of interpolation uncertainty.

2.6. Validation Technique/Accuracy Assessment

Two well-known methods for assessing interpolation accuracy and model overfitting are cross-validation [29,34–36] and the split-sample method [29,37–39]. In this study, the split-sample method was employed to evaluate how changes in line spacing affect interpolation accuracy. This method involves splitting the dataset into training and testing subsets, where the training data are used for interpolation, and performance is assessed using the test data. Standard statistical metrics such as RMSE, mean absolute error (MAE), bias, and R^2 are frequently used for evaluation [40–42]. RMSE and R^2 were applied in this study.

To evaluate the statistical significance of differences among interpolation methods, pairwise t-tests were conducted. These tests were used to compare uncertainties between pairs of interpolation methods and assess whether the differences were statistically different from zero. Notably, the normality of pairwise difference distribution was also checked. In addition to the statistical evaluation, visual inspection was conducted to spatially assess interpolation accuracy and understand the spatial distribution of uncertainty, providing a qualitative characterization of interpolation uncertainties.

3. Results

Interpolation Methods

The performance of the interpolation methods at each line spacing for each testbed is evaluated using box and whisker plots (Figures 7 and 8). Overall, the interpolation uncertainty from Spline was better than IDW and Linear, except in Testbed 1, where Linear yielded better results. IDW consistently showed the worst performance across all testbeds. Figures 7 and 8 illustrate the performance of the interpolation methods across all line spacings for Testbeds 1 and 4, which were selected for presentation due to their significant variation in uncertainty magnitude, encompassing the range of uncertainties observed in the other testbeds.

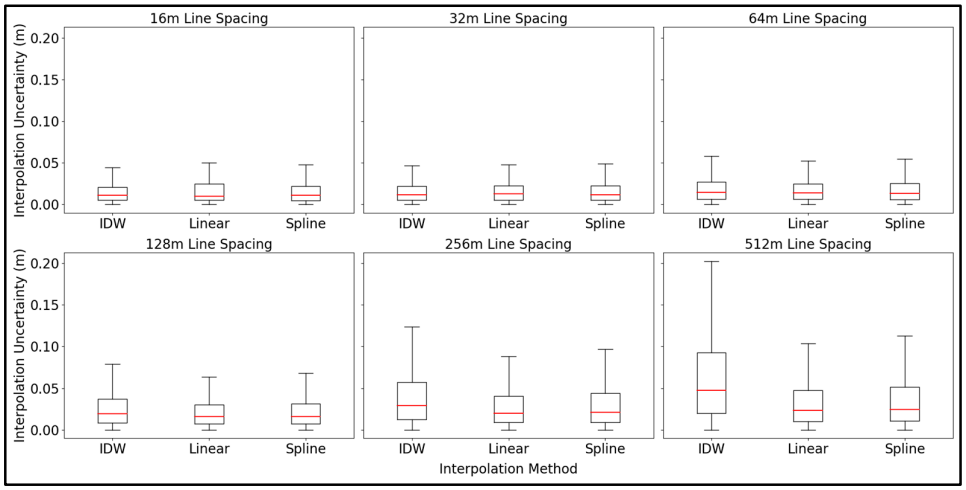

Figure 7. Testbed 1 interpolation methods' uncertainty comparison at various line spacings using boxes and whiskers, plotted with 99% percentile of data.

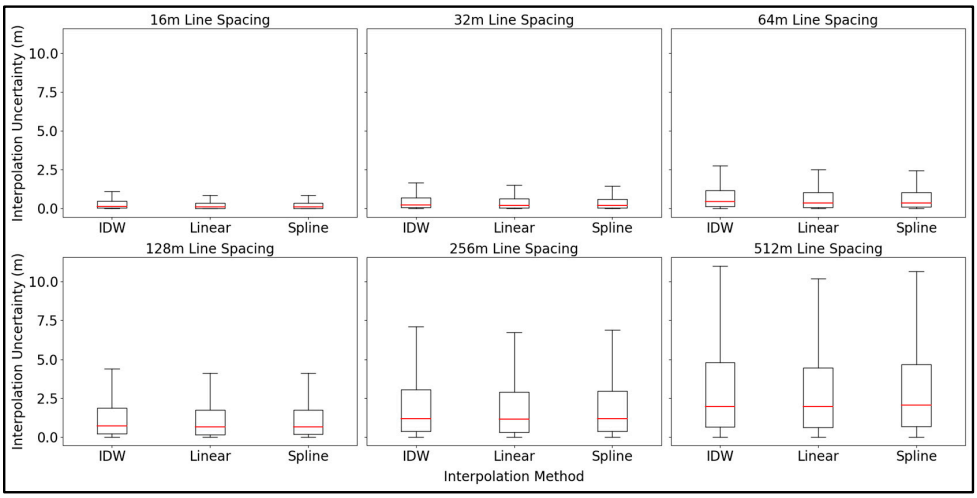

Figure 8. Testbed 4 interpolation methods' uncertainty comparison at various line spacings using boxes and whiskers, plotted with 99% percentile of data.

However, the above differences in interpolation methods across various line spacings for all testbeds are not statistically significant, as indicated by pairwise analysis. Figure 9 and Table 2 present the distribution of pairwise interpolation uncertainty differences and the *t*-test results for Testbed 4, which serves as a representative example of the other testbeds.

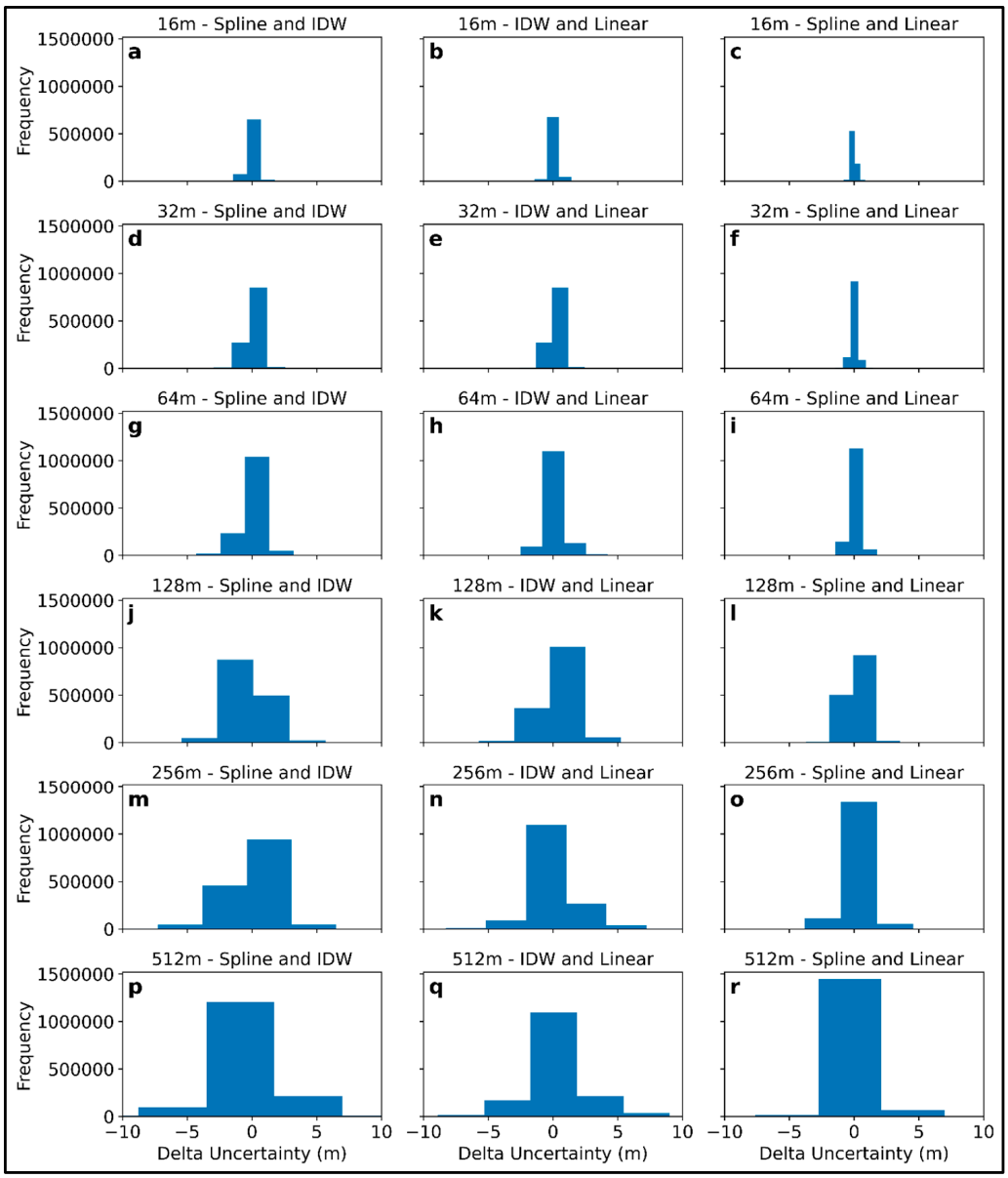

Figure 9. Histograms showing pairwise differences in interpolation methods' uncertainties for Testbed 4 (rough and slopy) at various line spacings.

Table 2. Testbed 4 (rough and slopy) statistics for pairwise interpolation methods' comparison at various line spacings.

Line Spacing (m)	Interpolation Methods	t-Statistics	*p*-Value
16	Spline and IDW	−160	0
	IDW and Linear	176.8	0
	Spline and Linear	−20.3	0

Table 2. *Cont.*

Line Spacing (m)	Interpolation Methods	t-Statistics	*p*-Value
32	Spline and IDW	−106.7	0
	IDW and Linear	113.4	0
	Spline and Linear	−22.5	0
64	Spline and IDW	−139.8	0
	IDW and Linear	153.4	0
	Spline and Linear	6	0
128	Spline and IDW	−111.8	0
	IDW and Linear	147.4	0
	Spline and Linear	59.6	0
256	Spline and IDW	−76.6	0
	IDW and Linear	140.4	0
	Spline and Linear	118.3	0
512	Spline and IDW	−53.9	0
	IDW and Linear	151.8	0
	Spline and Linear	171.9	0

The magnitude of interpolation uncertainties is in the order of centimeters for Testbeds 1 (Figure 7) and 2, whereas for the more complex Testbeds 3 and 4 (Figure 8), uncertainties are in the order of meters. Moreover, differences between uncertainties are relatively higher at wider line spacings across all testbeds, while at tighter line spacings, uncertainties tend to become the same.

a Spatial Pattern of Interpolation Uncertainties

The spatial pattern of the interpolation uncertainties refers to the distribution and arrangement of uncertainty values across the testbed, highlighting how they vary spatially in response to different predictors. In this study, these patterns were visually examined qualitatively across Testbeds 1 to 4 to understand how seafloor characteristics, distance to the nearest measurement, and data quality affect interpolation uncertainty. The results indicate that the uncertainties are not randomly distributed; instead, they follow specific, identifiable patterns based on seafloor characteristics, distance to the nearest measurement, and multibeam data artifacts (see Figures 10 and 11).

In Testbed 1, higher uncertainties are concentrated on the eastern side, likely due to multibeam artifacts in the original dataset. For Testbed 2, higher uncertainties are associated with areas of increased surface roughness. In Testbed 3, higher uncertainties are linked to regions with steeper slopes. Testbed 4 shows non-random patterns, with higher uncertainties correlating with both high slope and roughness values. Given the presence of multibeam artifacts in Testbed 1 and the larger uncertainty magnitudes in Testbed, their spatial uncertainty plots are shown in Figures 10 and 11, respectively. To ensure a meaningful comparison, the color bar has been standardized across all line spacings and interpolation methods. However, differences in the subplots at identical line spacings—viewed horizontally—are minimal due to the similar performance of the interpolation methods.

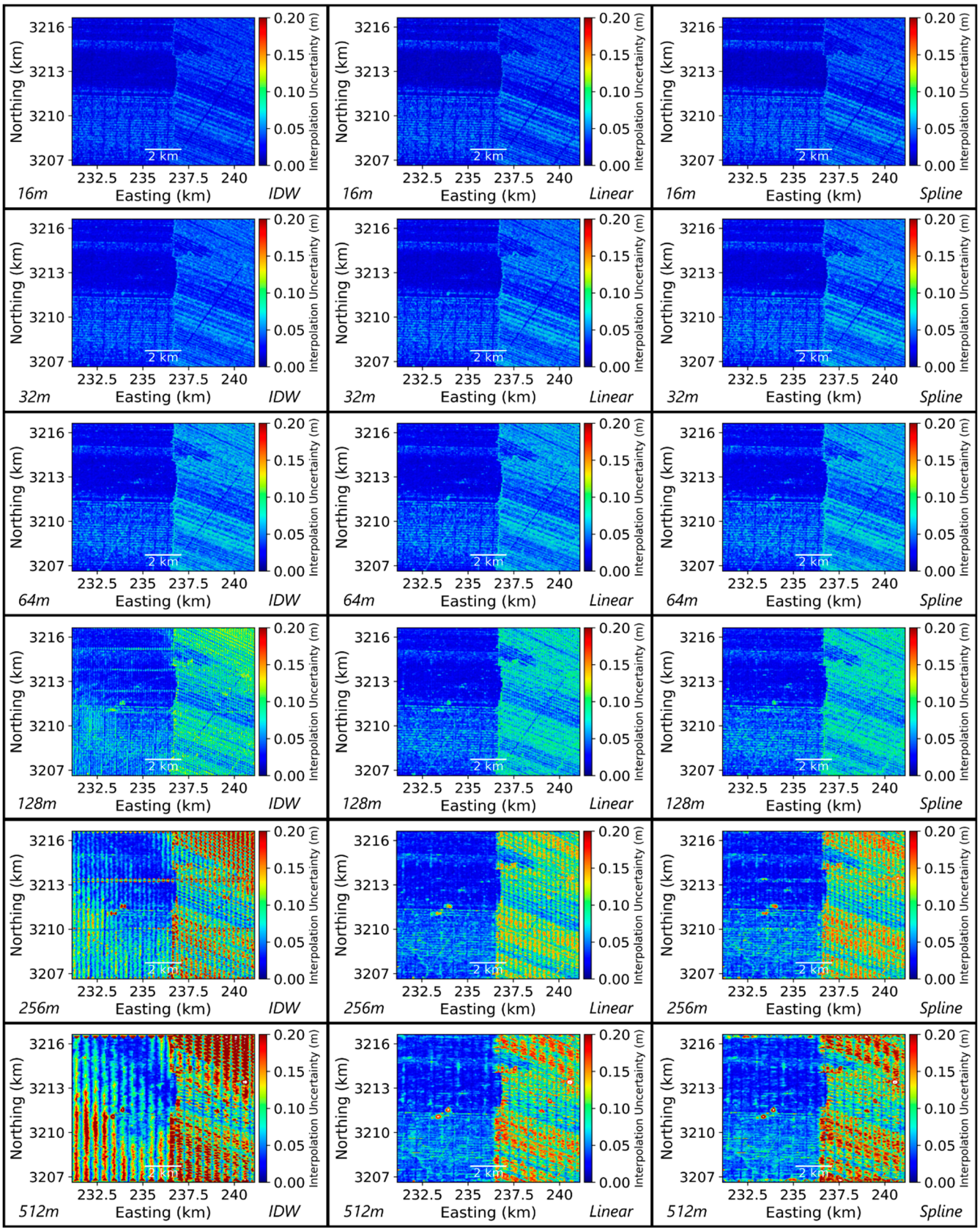

Figure 10. Testbed 1 interpolation uncertainty across all line spacings (columns) and interpolation methods (rows), using 99th percentile of data. Uncertainty values are presented in absolute terms.

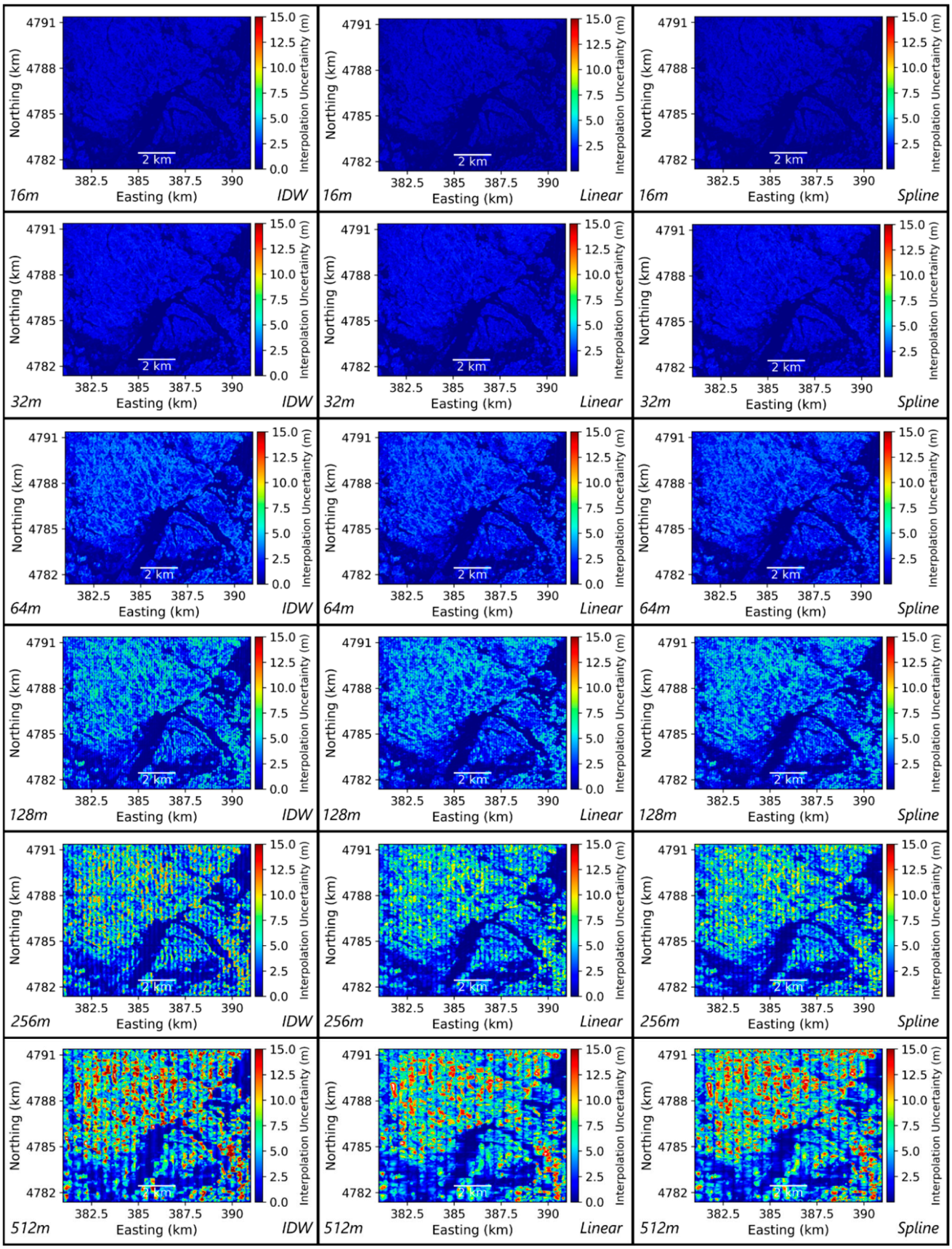

Figure 11. Testbed 4 interpolation uncertainty across all line spacings (columns) and interpolation methods (rows), using 99th percentile of data. Uncertainty values are presented in absolute terms.

b. Predictive Models of Interpolation Uncertainties

Across the testbeds, the linear regression relationships between interpolation uncertainty and individual ancillary predictors (i.e., distance to the nearest known measurement, slope, and roughness) were generally weak for all interpolation methods (see Figure 12). To explore potential nonlinearities and hidden interactions among these combined predictors and the estimated uncertainty, we employed an ANN. This resulted in a slight improvement in the adjusted R^2 (Figure 13), although the accuracy of the predictive models based on these combined predictors varied significantly across the testbeds. The highest performance was observed in Testbed 4, followed by Testbeds 3, 2, and 1.

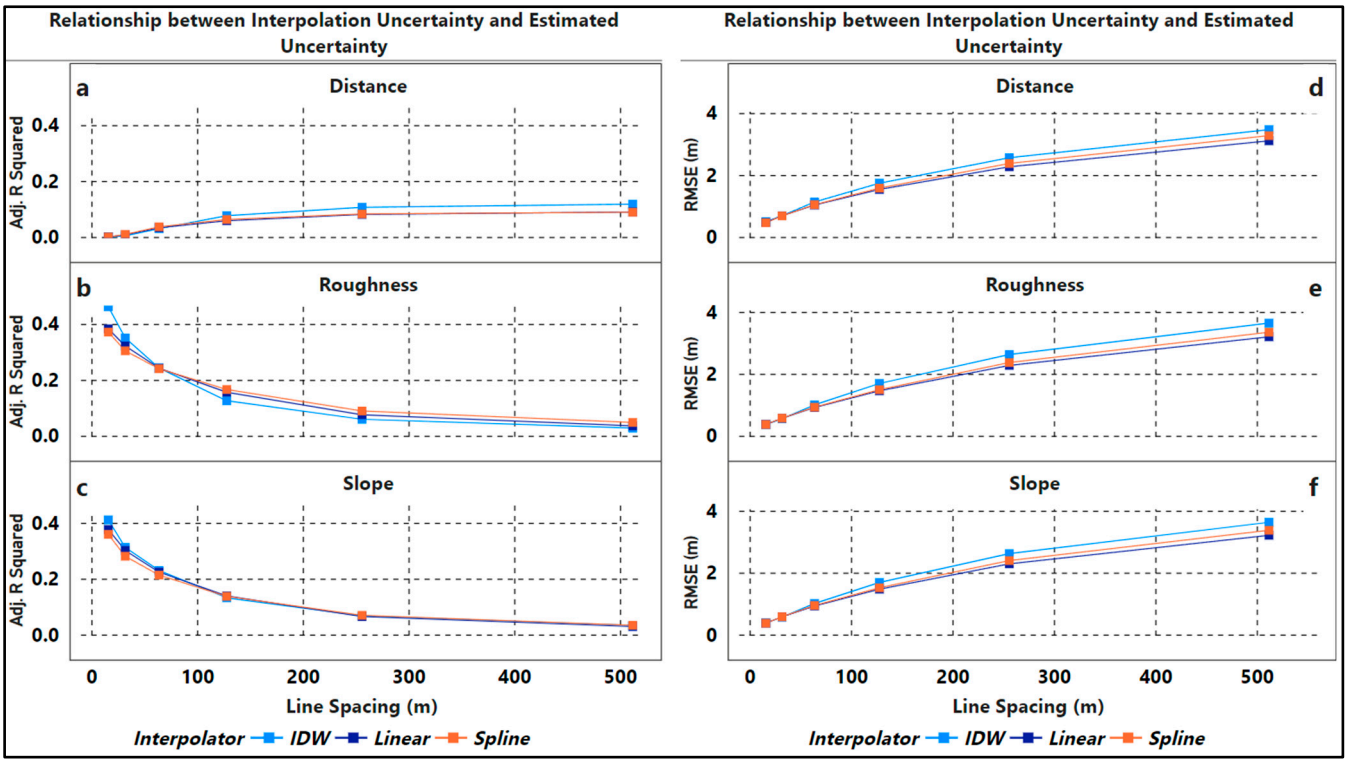

Figure 12. Adjusted R^2 (**a**–**c**) and RMSE (**d**–**f**) of the relationship between interpolated uncertainty and estimated uncertainty based on distance to nearest measurement, roughness, and slope, respectively, for Testbed 4.

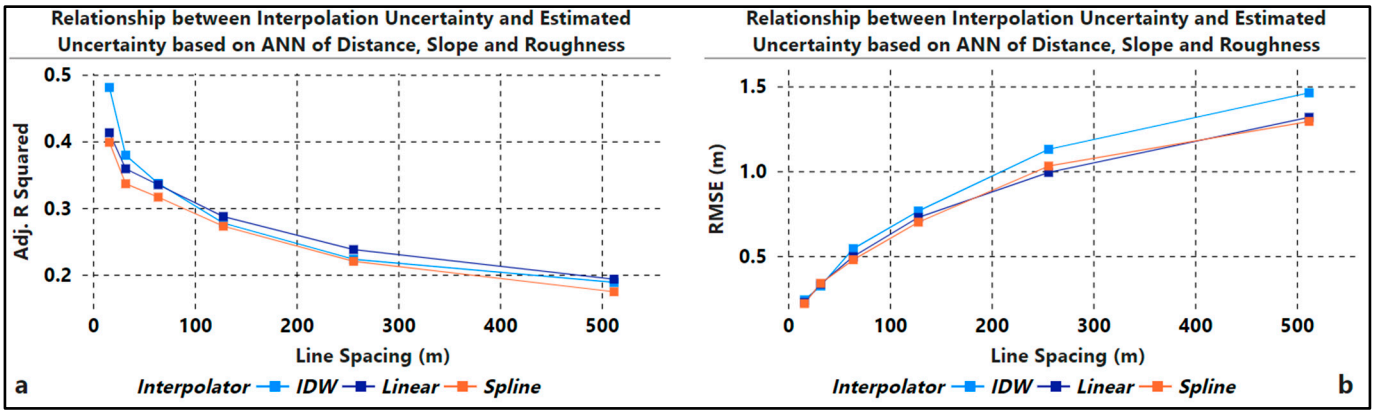

Figure 13. Adjusted R^2 (**a**) and RMSE (**b**) of the relationship between interpolated uncertainty and estimated uncertainty based on distance to nearest depth measurement, roughness, and slope combined for Testbed 4.

Among the interpolation techniques, IDW's predictive uncertainty model generally achieved higher adjusted R^2 values compared to those of Spline and Linear, but it had the worst performance in terms of RMSE. Spline and Linear interpolations showed similar performance for both metrics. Figures 12 and 13 present the predictive uncertainty models for Testbed 4, the best-performing testbed, for both individual and combined predictors. The differences in RMSE between the interpolation methods' predictive uncertainty models were in the order of centimeters, which are not operationally significant for meeting survey order or charting specifications. For instance, the 15 cm difference between Spline's and IDW's uncertainty model at a 512 m line spacing, as shown in Figure 13b, is not operationally significant. A 512 m line spacing survey would not be conducted in water depths where uncertainties of this magnitude would pose a hazard to navigation.

The results from the RF analysis, combined with the bootstrap statistical technique (Table 3), identified slope as the strongest predictor of uncertainty in Testbeds 1 and 2, while roughness emerged as the best predictor in Testbeds 3 and 4. Across all testbeds, distance to the nearest known measurement was found to be the least significant predictor of uncertainty.

Table 3. Statistics of the importance of predictors of uncertainty across testbeds.

Testbed	Statistics/Predictor	Distance	Slope	Roughness
1	Mean importance (%)	8.4	52.8	38.7
	# times of most important	0	13	5
	95% bootstrap percentile CI of the importance	(8.0, 8.8)	(51.4, 54.3)	(37.3, 40.1)
2	Mean importance (%)	11.5	49.7	38.8
	# times of most important	0	12	6
	95% bootstrap percentile CI of the importance	(11.1, 11.8)	(48.9, 50.5)	(38.0, 39.7)
3	Mean importance (%)	9.3	37.7	53.0
	# times of most important	0	3	15
	95% bootstrap percentile CI of the importance	(8.9, 9.7)	(36.2, 40.4)	(50.3, 54.5)
4	Mean importance (%)	8.8	38.3	52.9
	# times of most important	0	1	17
	95% bootstrap percentile CI of the importance	(8.5, 9.0)	(37.5, 39.1)	(52.2, 53.7)

4. Discussion

4.1. Unraveling the Contextual Performance of Interpolation Methods

The analysis of results revealed that, from a scientific standpoint—specifically in terms of minimizing uncertainty—Linear interpolation performed best for Testbed 1 (flat), while Spline performed best for Testbeds 2 (rough), 3 (sloped), and 4 (rough and sloped). IDW consistently showed the worst performance across all testbeds. However, when evaluated from an operational perspective and their effect to surface navigation, the interpolation methods performed similarly with differences in the range of centimeters. These are unlikely to affect the CATZOC designation due to the total depth vertical uncertainty (as shown in Table 1), particularly in shallow waters where the differences are nonexistent (see, e.g., Figure 13 for line spacing up to 256 m that corresponds to a water depth of, approximately, 64 m). The lack of statistically significant differences in the performance of interpolators indicates operational equivalence among the three interpolation methods. This suggests that linear interpolation may be the most suitable choice in operational settings, given its simplicity and lower computational demands.

Testbeds 1 and 2 exhibited uncertainties in the order of centimeters due to their relatively simpler morphologies as shown in Figure 2. In contrast, Testbeds 3 and 4, which

have more complex features, showed uncertainties in the order of meters, particularly at wider line spacings (256 m and 512 m). Even though Testbeds 1 to 4 have varying depth ranges, 26 m, 11 m, 140 m, 90 m, respectively, these differences in depth range do not impact the uncertainties results. This is justified by expressing uncertainties as a percentage of depth, and the same outcome was observed. To facilitate analysis and enhance result comprehension in this study, interpolation uncertainties are presented as absolute values. The variability in uncertainties indicates that seabed complexity has a significant impact on interpolation uncertainties, with Testbeds 1 (flat) and 2 (rough) yielding more accurate results compared to Testbeds 3 (slopy) and 4 (rough and slopy), especially in the context of creating DBMs from set-line spacing surveys and field operations. This finding emphasizes that seabed morphology should be one of the variables driving set-line spacing survey density. It also suggests that a set-line spacing survey approach is more suitable for simpler morphologies, as interpolation uncertainties can reach up to 15 m in 100 m of depth or more in complex morphologies, as shown in Figure 10.

The impact of line spacing is conspicuous, particularly in Testbeds 3 and 4, where uncertainties become relatively similar and smaller at tighter line spacings. This suggests that denser line spacing is a way of overcoming geomorphologically related uncertainty on Testbeds 3 and 4. Summarily, the interpolation method performance varies across testbeds, influenced by seabed morphology and line spacing. While nuanced differences exist, the overall insights suggest that selecting an interpolation method should be tailored to the specific characteristics of the seabed under consideration.

Additionally, the qualitative spatial analysis of interpolation uncertainties across the testbeds reveals distinct, non-random patterns. For instance, higher uncertainties are concentrated in specific regions, such as the eastern side of Testbed 1 (see Figure 10) due to the artifacts in the original dataset, and areas associated with high distances to the nearest known measurement and high slope or roughness values in Testbeds 2, 3, and 4. This highlights the influence of underlying terrain characteristics and line spacings on uncertainty. The multibeam artifacts present in Testbed 1 further illustrate how uncertainties from the original data can propagate into the interpolation process. The choice of this dataset with artifacts was to investigate the effect of multibeam artifacts on interpolation uncertainty. Even though survey data may be affected by multibeam artifacts, they may still meet the IHO specifications they were targeted for [43]. These findings underscore the interplay between data quality, line spacing density, seabed morphology complexity, and interpolation uncertainties.

In summary, the choice of interpolation method does not have a significant impact on results, and the differences in uncertainties are generally not statistically significant. The performance of interpolation methods varies across testbeds, suggesting that morphological complexity should guide the density of set-line spacing surveys. This means that in rougher and sloped terrains, such as those found in Testbeds 3 and 4, survey lines should be spaced more densely to reduce interpolation uncertainty, whereas less complex terrains allow for less dense spacing.

4.2. Relationship Among Predictors, Line Spacing, and Interpolation Uncertainty

Through varying line spacings, roughness was identified as the most important predictor of uncertainty for Testbeds 3 and 4, followed by slope and distance to the nearest known measurement. Conversely, for Testbeds 1 and 2, slope was the most significant predictor, with roughness and distance to the nearest known measurement following. The observed weak association among roughness and slope, as defined in this work, and distance to the nearest known measurement with interpolation uncertainty using the ANN highlights the complexity of estimating uncertainty in interpolated bathymetry. Machine learning does

improve the predictive capability of the model, yet the combined predictors explain only about, e.g., 40% of the variability in the data at a 16 m line spacing, as shown in Figure 13.

Distance to the nearest known measurement, being the least significant predictor of uncertainty, contributes minimally to the overall estimation, as evidenced by both linear regression and RF analysis. While distance shows a correlation with interpolation uncertainty at wider line spacings, its impact remains limited.

Despite the importance of slope and roughness as a predictor of interpolation uncertainty, their combined explanatory power is limited, as shown in [18], suggesting the presence of unaccounted-for factors influencing uncertainty or a strong random component within interpolation uncertainty. This outcome also suggests that the definitions of roughness and slope, which were based on spatial scales close to the seafloor sampling frequency, limited the range of the spatial scales of the analysis and contributed to the low predictive capabilities of the machine learning models.

Notably, the introduction of machine learning techniques in this work enhanced our understanding of the complexity of the problem and the weak relationship between interpolation uncertainty, and the combined ancillary predictors signaled the necessity for alternative approaches such as spectral analysis. This approach may help to better characterize the seafloor across varying spatial scales and improve the prediction of interpolation uncertainty. While additional predictors were considered, such as morphological aspects and curvature, they exhibited no discernible relationship with interpolation uncertainty as also found in [18] and, therefore, are not included in this study.

The slight improvement in the ANN's model performance at tighter line spacings across the testbeds underscores the importance of reasonable line spacings. Wider line spacings correspond to increased interpolation uncertainty, and vice versa. Additionally, as line spacing increases, the uncertainty model struggles to capture the subtle variations in seabed morphology, leading to a reduction in predictive capability. This finding accentuates the significance of strategic set-line survey designs, where appropriate line spacings can enhance the estimation of interpolation uncertainty. This has implications for real-world hydrographic surveys targeted at a particular CATZOC level to maximize survey efficiencies, cost, and time.

4.3. Examining Disparities in Testbed Predictive Performance of Interpolation Methods

The significant differences in predictive performance across the testbeds highlight the context-dependent nature of interpolation uncertainty. Testbed 4 (rough and slopy) demonstrated the highest predictive capability (though the lowest interpolation accuracy), likely due to the greater spatial variability inherent in rough and slopy seabeds, which may have contributed to a better model fit. The inclusion of slope and roughness as predictors likely enhanced the model's performance in Testbed 4.

Interestingly, Testbed 3 (slopy) performed nearly as well, with roughness identified as the primary predictor of uncertainty. This suggests that other unexamined factors may be influencing the results, underscoring the complexity of the relationship between these predictors and predictive performance.

Testbed 2 (rough) performed slightly worse than Testbed 3, with slope emerging as the most important predictor of uncertainty. This is likely due to the fact that the rough and slopy testbed has some interactive effect on slope and roughness. For example, Testbed 2, despite being defined as rough, has some slope in it. This suggests a disconnect between seabed characteristics and predictive capability, emphasizing the complexity of this relationship.

Finally, Testbed 1 (flat) showed the lowest predictive performance, affirming the challenge of capturing variability in less complex terrains.

These findings underscore the importance of considering the specific characteristics of the seabed when developing and applying interpolation models, recognizing the intricate interactions that influence predictive capability in diverse seabeds.

4.4. Importance of Predictors

A detailed analysis of the RF results, supported by the bootstrap statistical technique, revealed that roughness holds the highest predictive importance for interpolation uncertainty, followed by slope and distance to the nearest known measurement for Testbeds 3 and 4 while slope emerged as the most important predictor for Testbeds 1 and 2. Across all testbeds, the consistently low importance of distance to the nearest known measurement highlights its minimal contribution to the predictive models. In contrast, the strong influence of roughness and slope underscores the critical role that terrain characteristics play in shaping interpolation uncertainties.

Interestingly, on Testbeds 1 and 2, slope emerged as the most important predictor while competing with roughness, potentially due to the less complex morphology of these seabeds. Conversely, on the more complex Testbeds 3 and 4, roughness dominated as the key predictor. The use of the bootstrap statistical technique further supports the reliability of these findings, confirming the statistical significance of the differences observed among predictors.

Overall, these findings provide a deeper understanding of the key factors in predictive models of interpolation uncertainties for set-line spacing surveys. Recognizing the hierarchical importance of these predictors offers valuable insights into how uncertainty in interpolated bathymetry can be effectively quantified in such surveys.

4.5. Limitations of the Study

This study focused on estimating interpolation uncertainty in operational settings, where data-driven products are generated from large datasets. As a result, we excluded geostatistical interpolation methods like Kriging, which, though providing uncertainty estimates, are computationally demanding and require significant memory resources.

Additionally, the interpolation parameters used in our study were based on general values from the existing literature, rather than being optimized for the specific characteristics of each testbed. While parameter optimization might enhance accuracy, it was beyond the scope of this research.

This study also focused solely on the uncertainty related to depth accuracy in CATZOC, without addressing horizontal accuracy or factors related to seafloor feature detection, such as expected feature size or seabed undulations.

4.6. Future Research Directions

Exploring sophisticated alternatives, such as spectral analysis for uncertainty estimation, may advance this research area. While the results in this work do not model significant predictive power for the strict definitions of roughness and slope used here, the spatial scales associated with these definitions are closely tied to the spatial sampling frequency. Spectral analysis may facilitate analysis over a broader range of spatial frequencies and improve the model's predictive power. The integration of spectral analysis with machine learning techniques holds significant potential for improving interpolation uncertainty estimates and the detection of seafloor features.

In this study, we assumed that the depth data from BlueTopo were free of measurement uncertainty. However, it is important to recognize that depth measurements typically carry uncertainty due to various factors (refer to [44]). Future research should aim to integrate measurement uncertainty with interpolation uncertainty, which would enable a more accurate assignment of CATZOC values for nautical charting.

The testbeds in this study are confined to U.S. waters, although they address a useful range of morphological characteristics. This confinement does not limit the generalizability of the findings, as global nautical charting surveys adhere to the international guidelines set by the International Hydrographic Organization (IHO) (see [22]). Future work should expand to include broader geographic regions and diverse bathymetric characteristics to enhance the applicability of these findings. Another important avenue for future research is exploring how interpolation uncertainty can inform the optimization of set-line spacing in hydrographic survey design to meet desired CATZOC standards. Such optimization could improve survey efficiency in terms of both time and cost, while ensuring that the necessary accuracy standards are met. These multidimensional investigations have the potential to transform the methodologies used in hydrographic surveys.

Finally, future research should compare actual interpolation uncertainty with Kriging uncertainty. This is particularly relevant as the interpolation uncertainty statistics observed in this study diverge from key assumptions, such as homogeneity of variance, which are central to the Kriging method.

5. Conclusions

This study aimed to identify the best bathymetric gap-filling interpolation method—which minimizes interpolation uncertainty—and accurately quantify and characterize-uncertainty in set-line spacing surveys. It sought to establish the relationship between interpolation uncertainty and a suite of ancillary predictors—distance to the nearest known measurement, slope, and roughness—across four testbeds in the United States, using tighter and wider line spacings.

The findings revealed that Spline is the best interpolation method for Testbeds 2 (rough), 3 (slopy), and 4 (rough and slopy), followed by Linear and IDW. For Testbed 1, Linear interpolation resulted in the least interpolation uncertainty, followed by Spline and IDW. However, this study also showed the operational equivalence of accuracies produced by different interpolation methods, as the differences observed are generally negligible from an operational standpoint, reflecting uncertainties in centimeters that may not practically impact CATZOC designations.

The weak relationship between the interpolation uncertainty and the predictors, roughness, slope, and distance to the nearest known measurement highlighted the challenges in estimating uncertainty in set-line spacing surveys. This in turn impacts the ability to establish operational survey plans that will maximize accuracy for a minimum cost. The introduction of machine learning techniques to combine the predictors into a single ANN model provides marginal improvements, while RF reveals the dominance of roughness and slope as the most important predictors, across the testbeds. Additionally, IDW better captured the variability of interpolation uncertainty than the Spline and Linear methods for most testbeds. The impact of appropriate line spacing on an uncertainty model's explanatory power is evident, diminishing effectiveness with tighter line spacings and wider line spacings.

Moreover, the model performance varied across testbeds, with Testbed 4 (rough and slopy seabed) yielding the best results (R^2 of 0.4 at a 16 m line spacing), followed by Testbed 3 (slopy seabed), Testbed 2 (rough seabed), and Testbed 1 (flat seabed). These insights highlight the presence of unaccounted-for factors influencing uncertainty or a strong random component within interpolation uncertainty.

Although this research focused on deterministic interpolation methods, the decision not to optimize parameters for each testbed reflects the operational focus of the study, where processing time and limited parameter adjustments are prioritized. This research advances our understanding of how measurable factors contribute to uncertainty estimates in set-line

spacing surveys, offering valuable perspectives for uncertainty estimation, hydrographic survey planning, and future research and applications in this domain.

Author Contributions: Conceptualization, Elias Adediran, Christos Kastrisios, Kim Lowell, and Glen Rice; methodology, Elias Adediran, Christos Kastrisios, Kim Lowell, Glen Rice, and Qi Zhang; software, Elias Adediran; validation, Elias Adediran, Christos Kastrisios, Kim Lowell, Glen Rice, and Qi Zhang; formal analysis, Elias Adediran, Christos Kastrisios, Kim Lowell, Glen Rice, and Qi Zhang; investigation, Elias Adediran, Christos Kastrisios, Kim Lowell, Glen Rice, and Qi Zhang; resources, Elias Adediran, Christos Kastrisios, Kim Lowell, Glen Rice, and Qi Zhang; data curation, Elias Adediran and Glen Rice; writing—original draft preparation, Elias Adediran; writing—review and editing, Elias Adediran, Christos Kastrisios, Kim Lowell, Glen Rice, and Qi Zhang; visualization, Elias Adediran; supervision, Christos Kastrisios and Kim Lowell; project administration, Christos Kastrisios and Kim Lowell; funding acquisition, Christos Kastrisios and Kim Lowell. All authors have read and agreed to the published version of the manuscript.

Funding: The work was supported by the National Oceanic and Atmospheric Administration under grant number NA20NOS4000196.

Data Availability Statement: The original data presented in the study are openly available from FigShare at https://figshare.com/s/970f1b196515dea5c297 (accessed on 23 December 2024).

Acknowledgments: We express our gratitude to the National Bathymetric Source team at the National Oceanic and Atmospheric Administration's Office of the Coast Survey for their invaluable support throughout this study. Our thanks also go to Ioannis Kornaros for his constructive discussions and valuable insights into data analysis. Finally, we are grateful to the three anonymous reviewers whose thoughtful feedback enhanced the quality and clarity of this work.

Conflicts of Interest: The authors declare no conflicts of interest.

Appendix A

Table A1. Summary of testbeds. NAD83—North American Datum of 1983 and UTM—Universal Transverse Mercator.

Testbed	Name	Morphology	Locality	Depth Range (m)	BlueTopo Tiles	NAD83 UTM Zone
1	Flat	Low roughness and low slope	Gulf of Mexico, LA, USA	−26–−52	BF2G62KP_20230505 BF2G72KP_20230505	16 N
2	Rough	High roughness and low slope	Florida Main Channel, FL, USA	−17–−28	BH4ST58G_20230607 BH4ST58H_20230607 BH4SV58G_20221125 BH4SV58H_20221125	17 N
3	Slopy	High slope and low roughness	Massa-chusetts Bay, MA, USA	−60–−200	BF2JK2MD_20230614	19 N
4	Rough and Slopy	High slope and high roughness	Gulf of Maine, ME, USA	−12–−102	BF2JK2MH_20230626 BF2JK2MG_20230418	19 N

References

1. Weatherall, P.; Marks, K.M.; Jakobsson, M.; Schmitt, T.; Tani, S.; Arndt, J.E.; Rovere, M.; Chayes, D.; Ferrini, V.; Wigley, R. A new digital bathymetric model of the world's oceans. *Earth Space Sci.* **2015**, *2*, 331–345. [CrossRef]
2. Smith, W.H.F. Introduction to this special issue on bathymetry from space. *Oceanography* **2004**, *17*, 6–7. [CrossRef]
3. Smith, W.H.F.; Sandwell, D.T. Global sea floor topography from satellite altimetry and ship depth soundings. *Science (1979)* **1997**, *277*, 1956–1962. [CrossRef]
4. Mayer, L.; Jakobsson, M.; Allen, G.; Dorschel, B.; Falconer, R.; Ferrini, V.; Lamarche, G.; Snaith, H.; Weatherall, P. The Nippon Foundation—GEBCO Seabed 2030 Project: The Quest to See the World's Oceans Completely Mapped by 2030. *Geosciences* **2018**, *8*, 63. [CrossRef]

5. Nippon Foundation-GEBCO. Our Mission—Seabed 2030. Available online: https://seabed2030.org/our-mission/ (accessed on 30 June 2023).
6. Wölfl, A.-C.; Snaith, H.; Amirebrahimi, S.; Devey, C.W.; Dorschel, B.; Ferrini, V.; Huvenne, V.A.I.; Jakobsson, M.; Jencks, J.; Johnston, G.; et al. Seafloor Mapping—The Challenge of a Truly Global Ocean Bathymetry. *Front. Mar. Sci.* **2019**, *6*, 283. [CrossRef]
7. Mayer, L. Frontiers in Seafloor Mapping and Visualization. *Mar. Geophys. Res.* **2006**, *27*, 7–17. [CrossRef]
8. Glenn, M.F. Introducing an operational multi-beam array sonar. *Int. Hydrogr. Rev.* **1970**, *47*, 35–39.
9. Renard, V.; Allenou, J.-P. Sea Beam, Multi-Beam Echo-Sounding in "Jean Charcot"-Description, Evaluation and First Results. *Int. Hydrogr. Rev.* **1979**, *56*. Available online: https://api.semanticscholar.org/CorpusID:131231796 (accessed on 23 December 2024).
10. Lurton, X. Swath bathymetry using phase difference: Theoretical analysis of acoustical measurement precision. *IEEE J. Ocean. Eng.* **2000**, *25*, 351–363. [CrossRef]
11. Irish, J.L.; White, T.E. Coastal engineering applications of high-resolution lidar bathymetry. *Coast. Eng.* **1998**, *35*, 47–71. [CrossRef]
12. Pe'eri, S.; Parrish, C.; Azuike, C.; Alexander, L.; Armstrong, A. Satellite Remote Sensing as a Reconnaissance Tool for Assessing Nautical Chart Adequacy and Completeness. *Mar. Geod.* **2014**, *37*, 293–314. [CrossRef]
13. IHO. Guidance to Crowdsourced Bathymetry. 2022. Available online: https://iho.int/uploads/user/pubs/bathy/B_12_CSB-Guidance_Document-Edition_3.0.0_Final.pdf (accessed on 28 July 2024).
14. NOAA OCS. Hydrographic Survey Specifications and Deliverables. 2022. Available online: https://nauticalcharts.noaa.gov/publications/docs/standards-and-requirements/specs/HSSD_2022.pdf (accessed on 13 November 2022).
15. Burrough, P.A.; McDonnell, R.A. *Principles of Geographical Information Systems*; Oxford University Press: Oxford, UK, 1998.
16. Liu, X.; Zhang, Z.; Peterson, J.; Chandra, S. LiDAR-derived high quality ground control information and DEM for image orthorectification. *Geoinformatica* **2007**, *11*, 37–53. [CrossRef]
17. Tobler, W.R. A Computer Movie Simulating Urban Growth in the Detroit Region. *Econ. Geogr.* **1970**, *46*, 234–240. [CrossRef]
18. Adediran, E.; Lowell, K.; Kastrisios, C.; Rice, G.; Zhang, Q. Exploring Ancillary Parameters for Quantifying Interpolation Uncertainty in Digital Bathymetric Models. *Mar. Geod.* **2024**, *47*, 289–323. [CrossRef]
19. Negreiros, J.; Painho, M.; Aguilar, F.; Aguilar, M. Geographical Information Systems Principles of Ordinary Kriging Interpolator. *J. Appl. Sci.* **2010**, *10*, 852–867. [CrossRef]
20. Gunarathna, M.H.J.P.; Nirmanee, K.G.S.; Kumari, M.K.N. Are Geostatistical Interpolation Methods Better than Deterministic Interpolation Methods in Mapping Salinity of Groundwater? *Int. J. Res. Innov. Earth Sci.* **2016**, *3*, 59–64.
21. Childs, C. Interpolating Surfaces in ArcGIS Spatial Analyst. In *ArcUser*; ESRI Press: Redlands, CA, USA, 2004.
22. IHO. International Hydrographic Organization Standards for Hydrographic Surveys S-44 Edition 6.0.0. 2020. Available online: www.iho.int (accessed on 18 September 2022).
23. IHO. IHO Transfer Standard for Digital Hydrographic Data Publication S-57. 2014. Available online: https://iho.int/uploads/user/pubs/standards/s-57/31Main.pdf (accessed on 18 September 2022).
24. IHO. International Hydrographic Organization S-101 Annex A, Data Classification and Encoding Guide. no. 1.0.2.2022. Available online: https://iho.int/ (accessed on 18 September 2022).
25. IHO. S-68 Guidelines and Recommendations for HOs for the Allocations of CATZOC/QOBD Values from Survey Data. 2023. Available online: www.iho.int (accessed on 9 October 2024).
26. Rice, G.; Wyllie, K.; Gallagher, B.; Geleg, P. The National Bathymetric Source. In Proceedings of the OCEANS 2023—MTS/IEEE U.S. Gulf Coast, Biloxi, MS, USA, 25-28 September 2023; pp. 1–7. [CrossRef]
27. Wilson, M.F.J.; O'Connell, B.; Brown, C.; Guinan, J.C.; Grehan, A.J. Multiscale Terrain Analysis of Multibeam Bathymetry Data for Habitat Mapping on the Continental Slope. *Mar. Geod.* **2007**, *30*, 3–35. [CrossRef]
28. Horn, B.K.P. Hill shading and the reflectance map. *Proc. IEEE* **1981**, *69*, 14–47. [CrossRef]
29. Amante, C.J.; Eakins, B.W. Accuracy of interpolated bathymetry in digital elevation models. *J. Coast. Res.* **2016**, *76*, 123–133. [CrossRef]
30. Agatonovic-Kustrin, S.; Beresford, R. Basic concepts of artificial neural network (ANN) modeling and its application in pharmaceutical research. *J. Pharm. Biomed. Anal.* **2000**, *22*, 717–727. [CrossRef] [PubMed]
31. Lundberg, S.; Lee, S.-I. A Unified Approach to Interpreting Model Predictions, in Neural Information Processing Systems. May 2017. Available online: https://api.semanticscholar.org/CorpusID:21889700 (accessed on 23 December 2024).
32. Agarap, A.M.F. Deep Learning Using Rectified Linear Units (ReLU). 2018. Available online: https://github.com/AFAgarap/relu-classifier (accessed on 12 November 2023).
33. Kingma, D.P.; Ba, J. Adam: A Method for Stochastic Optimization. CoRR, vol. abs/1412.6980. 2014. Available online: https://api.semanticscholar.org/CorpusID:6628106 (accessed on 23 December 2024).
34. Erdogan, S. A comparision of interpolation methods for producing digital elevation models at the field scale. *Earth Surf. Process. Landf.* **2009**, *34*, 366–376. [CrossRef]
35. Davis, B.M. Uses and abuses of cross-validation in geostatistics. *Math. Geol.* **1987**, *19*, 241–248. [CrossRef]

36. Tomczak, M.T. Spatial Interpolation and its Uncertainty Using Automated Anisotropic Inverse Distance Weighting (IDW)—Cross-Validation/Jackknife Approach. 1998. Available online: https://api.semanticscholar.org/CorpusID:14376667 (accessed on 23 December 2024).
37. Lloyd, C.D.; Atkinson, P.M. Deriving DSMs from LiDAR data with kriging. *Int. J. Remote Sens.* **2002**, *23*, 2519–2524. [CrossRef]
38. Voltz, M.; Webster, R. A comparison of kriging, cubic splines and classification for predicting soil properties from sample information. *J. Soil Sci.* **1990**, *41*, 473–490. [CrossRef]
39. Declercq, F.A.N. Interpolation Methods for Scattered Sample Data: Accuracy, Spatial Patterns, Processing Time. *Cartogr. Geogr. Inf. Syst.* **1996**, *23*, 128–144. [CrossRef]
40. Isaaks, E.H.; Srivastava, R.M. *An Introduction to Applied Geostatistics*; Oxford University Press: New York, NY, USA, 1989.
41. Li, J.; Heap, A.D. *A Review of Spatial Interpolation Methods for Environmental Scientists*; Geoscience Australia: Canberra, Australia, 2008.
42. Zar, J.H. *Biostatistical Analysis*; Prentice Hall: Edgewood Cliffs, NJ, USA, 1999.
43. Clarke, J.E.H.; Mayer, L.A.; Wells, D.E. Shallow-water imaging multibeam sonars: A new tool for investigating seafloor processes in the coastal zone and on the continental shelf. *Mar. Geophys. Res.* **1996**, *18*, 607–629. [CrossRef]
44. Hare, R.; Eakins, B.; Amante, C. Modelling Bathymetric Uncertainty. *Int. Hydrogr. Rev.* **2011**, 31–42. Available online: https://api.semanticscholar.org/CorpusID:56273262 (accessed on 23 December 2024).